

A MODEL FOR THE PERFORMANCE OF AIR-BREATHING PULSE DETONATION ENGINES

E. Wintenberger and J.E. Shepherd
*Graduate Aeronautical Laboratories,
 California Institute of Technology, Pasadena, CA 91125*

An analytical model for predicting the performance of a single-tube air-breathing pulse detonation engine has been developed. The model is based on control volume methods and elementary gas dynamics. The pulse detonation engine considered consists of a steady supersonic inlet, a large plenum, and a straight detonation tube (no exit nozzle). The filling process is studied in detail through numerical simulations, due to its influence on the initial conditions for detonation initiation. Control volume analysis and gas dynamics are used to model the coupled flow between the plenum and the detonation tube. It is shown that the average pressure in the plenum is lower than the stagnation pressure downstream of the inlet due to the unsteadiness of the flow, and that the flow in the plenum oscillates due to valve opening and closing. Moreover, the filling process generates a moving flow into which the detonation has to initiate and propagate. Our existing single-cycle impulse model is extended to include the effect of filling velocity on detonation tube impulse. Based on this, the engine thrust is calculated using an open-system control volume analysis. It is found to be the sum of the contributions of detonation tube impulse, ram momentum, and ram pressure. Performance calculations are carried out for pulse detonation engines operating with stoichiometric hydrogen-air and JP10-air and compared to the performance of the ideal ramjet.

Nomenclature

A_0	effective inlet capture area	P_R	initial pressure ratio across valve in numerical simulations of filling process
A_2	plenum cross-sectional area	P_t	stagnation pressure
A_V	valve and detonation tube cross-sectional area	q	heat release per unit mass
c	speed of sound	R	perfect gas constant
C_P	specific heat at constant pressure	t	time
e	internal energy	t_{CJ}	time taken by the detonation to reach the open end of the tube in the static case $= L/U_{CJ}$
f	fuel-air mass ratio	t_{close}	valve close time
F	thrust	t_{fill}	filling time
g	Earth's gravitational acceleration	t_{open}	valve open time
h_t	stagnation enthalpy per unit mass	t_{purge}	purging time
I_{dt}	detonation tube impulse	T	static temperature
I_{SPF}	fuel-based specific impulse	T_t	stagnation temperature
I_{SPFdt}	detonation tube fuel-based specific impulse	u	flow velocity
L	detonation tube length	U_{CJ}	detonation wave velocity
\dot{m}	mass flow rate	U_{fill}	filling velocity
\dot{m}_{Cin}	incoming mass flow rate	V	detonation tube volume
\dot{m}_{Cout}	outgoing mass flow rate	V_C	plenum volume
\dot{m}_f	average fuel mass flow rate	Z	altitude
\dot{m}_s	mass flow rate through side surfaces of control volume	α	non-dimensional parameter corresponding to time taken by first reflected characteristic to reach thrust surface
M	Mach number	β	non-dimensional parameter corresponding to pressure decay period
M_{fill}	filling Mach number	γ	ratio of specific heats
M_S	Mach number of the shock wave generated at valve opening in the burned gases	\mathcal{M}	mass of fluid in control volume
P	static pressure	Ω	engine control volume

π	purging coefficient
ρ	density
Σ	engine control surface
τ	cycle time

Subscripts

0	freestream
2	state downstream of inlet
3	state behind Taylor wave during detonation process
C	acoustic cavity (or plenum)
CJ	Chapman-Jouguet
f	state of detonation products at the end of blowdown process
i	state of reactants before detonation initiation at the end of filling process
dt	detonation tube
V	valve plane
*	state at valve plane when choked during filling process
o	model value during open part of cycle

Averages

\bar{X}	temporal average of X over a cycle
-----------	--------------------------------------

Introduction

Pulse detonation engines (PDEs) are propulsion systems based on the intermittent use of detonative combustion. Because of the intrinsically unsteady nature of the flow field associated with the detonation process, it is difficult to evaluate the relative performance of air-breathing PDEs with respect to conventional steady-flow propulsion systems.

PDE performance analysis has followed several different approaches. Researchers started by measuring¹⁻⁵ and modeling^{3,6-8} the static performance of single-cycle detonation tubes. In parallel, researchers have also investigated experimentally the static multi-cycle performance of single^{3,9} and multiple¹⁰ detonation tubes.

In contrast to the numerous studies carried out on the static performance of a PDE, very few efforts have focused on estimating the performance of an air-breathing PDE. The difficulties associated with coupling the inlet flow with the unsteady flow in the detonation tubes, and the lack of common understanding about the influence of nozzles on static PDE performance,¹¹ are some of the difficult obstacles to such modeling. Wu et al.¹² have presented what is so far the most comprehensive system performance analysis for an air-breathing hydrogen-fueled PDE, based on a modular approach including supersonic inlet dynamics and detonation in single and multiple tubes. Ma et al.¹³ recently extended this work to the thrust chamber dynamics of multiple-tube PDEs and obtained specific impulses as high as 3800 s with a single

converging-diverging exit nozzle. However, it is not clear how the interaction and coupling of the modules were treated in these models.

Other propulsion performance estimates for PDEs have been based on thermodynamic cycle analysis similar to those used in conventional steady propulsion systems, following the detonation thermodynamic cycle¹⁴ or a surrogate constant volume combustion cycle.¹⁵ Other models based on gas dynamics have been proposed.¹⁶ Harris et al.¹⁷ showed that the model proposed by Talley and Coy¹⁶ offers a good approximation of the time-averaged PDE performance, whereas the Heiser and Pratt analysis¹⁴ was shown to be overly optimistic in its prediction of PDE performance.

Because of the inherent unsteadiness associated with the detonation process and the pulsed operation of the PDE, the most successful performance models^{3,7,16} so far have been based on unsteady gas dynamics. We propose that PDEs have to be analyzed in an unsteady fashion, using open-system control volume analysis. Our goal is to develop a simple predictive model that can be used for engine performance evaluation at various operating conditions. We present a fully unsteady one-dimensional control volume analysis of a PDE, taking into account the kinetic energy terms, which are critical for high-speed propulsion systems. We focus on the modeling of a single-tube PDE, which includes an acoustic cavity that is large enough to minimize pressure transients associated with pulsed operation. We investigate in detail the flow field inside the engine, including the dynamics of the detonation tube, the acoustic cavity, and the inlet response. We perform an unsteady control volume analysis of the PDE. The conservation equations for mass, momentum, and energy are integrated over a cycle, and performance parameters are derived as a function of flight and operating conditions. Finally, the performance of a single-tube air-breathing PDE is compared with that of a conventional propulsion system, the ideal ramjet.

General considerations

Conventional steady inlets are attractive for PDE applications because their performance characteristics are well understood. They can be used in an unsteady air-breathing engine such as a PDE as long as the flow downstream of the inlet is quasi-steady. There are two ways to achieve quasi-steady state at the inlet. The first one is to design an inlet manifold large enough to dampen pressure transients and bleed excess air between detonation cycles. This approach requires an increased engine total volume and may not be practical. The second way is to use multiple detonation tubes operating out of phase so that the flow upstream of the detonation tubes is decoupled from the unsteady flow inside the tubes, and approaches quasi-steady state. The first approach is used in our modeling of the single-tube PDE.

The air-breathing PDE we consider in this paper consists of an inlet, a large acoustic cavity (or plenum), a valve, which is assumed to open and close instantaneously, and a detonation tube with fuel injectors. A schematic of a single-tube PDE with a steady inlet is illustrated in Fig. 1. The inlet, operating in a steady mode, is separated from the detonation tube by an isolator (a grid or screen similar to what is used in ramjets) and a large acoustic cavity, whose role is to protect the inlet from downstream flow perturbations due to combustion or valve motion. The detonation tube is assumed to be straight. As there is no wide agreement on the influence of nozzles on PDE performance, the effect of exit nozzles on detonation tube performance will not be considered in this initial study.

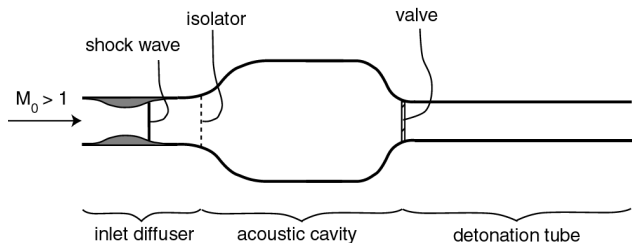


Fig. 1 Schematic representation of a single-tube pulse detonation engine.

Detonation tube dynamics

Before calculating the performance of a PDE, it is instructive to study the dynamics of the detonation tube during one cycle. A cycle has three main components: detonation and blowdown of burned gases, purging of the expanded burned products, and refilling of the tube with fresh reactants. Experiments have shown that purging the burned gases (usually with air) was a necessary precaution to avoid pre-ignition of the fresh mixture before the detonation is initiated. Fig. 2 illustrates the complete cycle for a given detonation tube, which is described in more detail in the following sub-sections. Fuel is injected in the low-speed flow upstream of the valve plane and is assumed to mix instantaneously with the flowing air. Total pressure losses associated with fuel-air mixing are neglected in our idealized model. The cycle time is the sum of the valve close time and the open time, the latter being the sum of the fill time and the purging time:

$$\tau = t_{close} + t_{open} = t_{close} + t_{fill} + t_{purge} \quad (1)$$

Although the unsteady flow in the detonation tube is complex and involves many wave interactions, the main physical processes occurring during a cycle are fairly obvious from previous studies.

Detonation/blowdown process

Detonation is assumed to be instantaneously directly initiated in the initial mixture at the closed end of the tube. The specific detonation tube dynamics

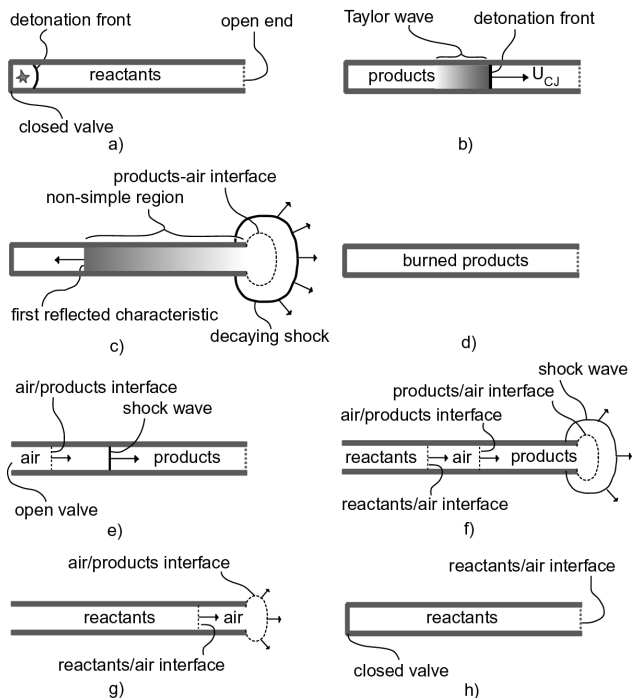


Fig. 2 PDE cycle schematic for a detonation tube. a) The detonation is initiated at the closed end of the tube. b) The detonation propagates towards the open end. c) The detonation diffracts outside as a decaying shock and a reflected expansion wave propagates to the closed end, starting the blowdown process. d) At the end of the blowdown process, the tube contains burned products at rest. e) The purging/filling process is triggered by the opening of the valve, sending a shock wave in the burned gases, followed by the air/products contact surface. f) A slug of air is injected before the reactants for purging. g) The purging air is pushed out of the tube by the reactants. h) The reactants eventually fill the tube completely and the valve is closed.

during the detonation process were studied in detail by Wintenberger et al.⁷ in the static case. It was shown that, as the detonation exits the tube, a reflected expansion wave propagates back towards the closed valve for hydrocarbon-air and lean and slightly rich hydrogen-air mixtures. After interacting with the Taylor wave, this reflected expansion decreases the pressure at the closed end of the tube and accelerates the fluid towards the open end. The pressure inside the tube typically decreases below the ambient pressure³ at the end of the blowdown process before going back up to ambient pressure after about $20t_{CJ}$. This suggests that the time during which the valve is closed for a given tube in an air-breathing PDE has to be at least $10t_{CJ}$ for maximized impulse per cycle.

In an air-breathing configuration, the flow in the detonation tube has a slightly different behavior because of the interaction of the detonation and filling processes. The valve is assumed to close instan-

taneously prior to the beginning of the detonation process. The valve closing sends an expansion wave through the tube to decelerate the flow created by the filling process. This expansion wave decreases the pressure and density inside the tube, which will decrease the detonation pressure, decreasing the thrust. If the detonation is assumed to be initiated as soon as the valve closes, it will overtake the expansion wave within the tube and propagate into the uniform flow produced by the filling process. The thrust for this situation will be different from the case of a detonation propagating into a stationary mixture but can be calculated if we assume ideal valve closing and detonation initiation.

Purging/filling process

At the end of the detonation/blowdown process, the valve at the upstream end of the tube, which was closed during the detonation/blowdown process, opens instantaneously. The opening of the valve triggers the expansion of the high-pressure air into the detonation tube containing burned gases at ambient pressure and elevated temperature. A shock wave is generated and propagates into the detonation tube, followed by the contact surface between fresh air and burned products. Fuel is typically not injected in the initial part of the filling process because purging the burned gases with air is required in order to avoid pre-ignition of the fresh mixture. An unsteady expansion wave propagates upstream of the valve inside the acoustic cavity and sets up a steady expansion of the cavity air into the detonation tube. The filling process is characterized by a combination of unsteady and steady expansions.

The gas dynamics of the flow are complex and involve multiple wave interactions, but in the interest of simplicity, we will attempt to characterize the filling process with a few key quantities. In order to do so, this problem was simulated numerically using Amrita.¹⁸ The simulations employed the non-reactive Euler equations in a two-dimensional domain with cylindrical symmetry, using a Kappa-MUSCL-HLLE solver. The configuration tested, shown in Fig. 3, consists of a large cavity connected by a smooth area change to a straight tube open to a half-space. The simulation was started with high-pressure air in the cavity at conditions given by $P_C/P_0 = P_R$, $T_C/T_0 = P_R^{(\gamma-1)/\gamma}$, separated from burned gases in the tube at pressure P_0 and elevated temperature $T_f = 7.69T_0$, representative of the temperature of the burned gases at the end of the blowdown process. The air outside the detonation tube is at pressure P_0 and temperature T_0 . The problem has two contact surfaces, the inlet air-burned gas interface at the valve end, and the burned gas-outside air interface at the tube exit. Numerical Schlieren images of the filling process are given in Fig. 3.

When the shock wave reaches the open end of the

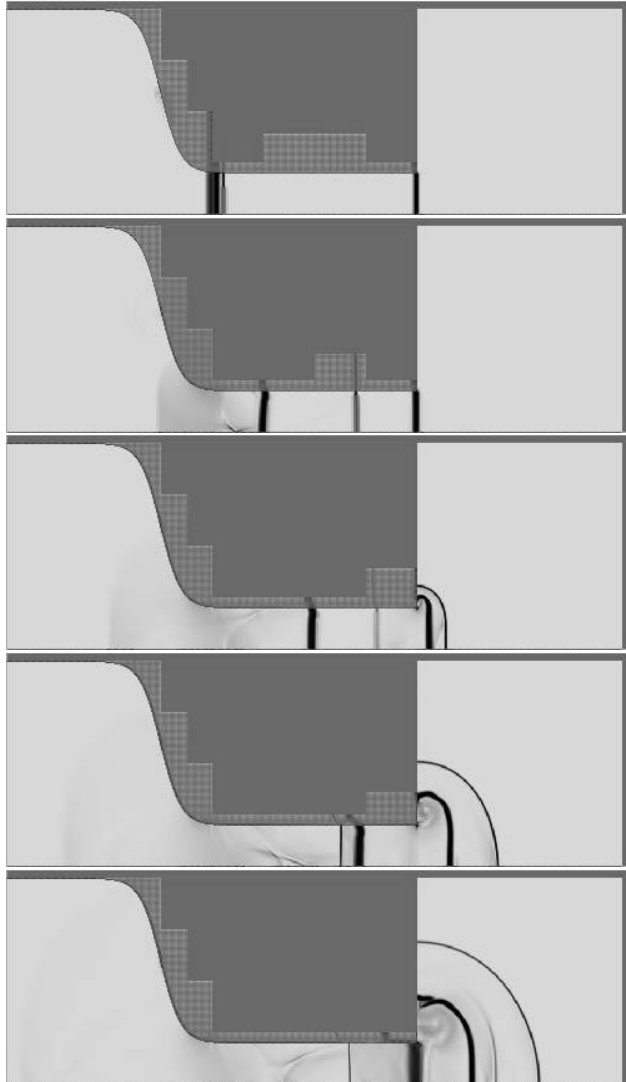


Fig. 3 Numerical Schlieren images of the filling process. $P_R = 8$, $T_f/T_0 = 7.69$, $\gamma = 1.4$.

detonation tube, it diffracts outwards, eventually becoming a decaying spherical shock, but also generates a reflected shock, due to the lower density of the burned products in the detonation tube than the outside air (soft-hard interaction). The reflected shock propagates upstream, interacting with the expansion waves that propagate back into the tube from the corners. The weakened shock then interacts with the inlet air-burned gas contact surface, generating a transmitted shock and a reflected expansion wave propagating towards the open end of the tube. When the flow behind the inlet air-burned gas contact surface is supersonic (for high values of P_R), the transmitted shock can be steady or also be convected by the flow towards the open end.

Although this problem is essentially multi-dimensional, the simulation results show that for pressure ratios low enough ($P_R < 5$), the flow inside the tube is essentially one-dimensional, except within one tube diameter of the tube exit, just

after the exhaust of the incident shock, when the multi-dimensional corner expansion waves propagate back into the tube. These waves quickly catch up and merge with the reflected shock. The subsequent reflected shock-contact discontinuity interaction appears one-dimensional. The same behavior is observed at higher pressure ratios, although two-dimensional waves generated by the starting process closely follow the inlet air-burned gas contact surface (Fig. 3).

Plenum/detonation tube coupling

The acoustic cavity (or plenum) is connected on one side to the steady inlet and on the other side to the unsteady valve at the front of the detonation tube. The conditions in the plenum and the flow in the detonation tube are coupled. The unsteady flow generated by the valve opening during the filling process depends on the conditions in the plenum and in the tube at the end of the detonation process but, in turn, affects the flow in the plenum. It is, therefore, critical to be able to model accurately the average conditions in the plenum.

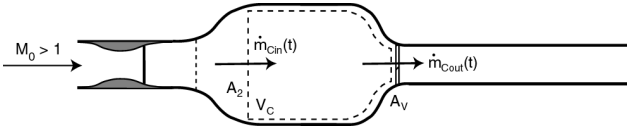


Fig. 4 Control volume V_C considered for analysis of flow in the plenum.

We assume that the cycle time is much larger than the characteristic acoustic transit time in the plenum so that the properties in the cavity can be modeled as spatially uniform. Assuming that the flow through the inlet diffuser is choked, the incoming mass flow rate in the plenum $\dot{m}_{Cin}(t)$ is constant and equal to \dot{m}_0 . The outgoing mass flow rate is defined as the flow rate at the valve plane $\dot{m}_V(t)$ when the valve is open. We are seeking the average conditions in the plenum, which determine the average filling conditions. In order to do so, we average over a cycle the mass, momentum, and energy conservation equations for the control volume V_C defined on Fig. 4. Although there is unsteady mass, momentum and energy variation during a cycle, there can be no accumulation in the plenum over a cycle during periodic operation. This yields

$$\overline{\dot{m}_V(t)} = \dot{m}_0 \quad (2)$$

$$\overline{\dot{m}_V(t)u_V(t)} = A_2 P_{t2} - A_V \overline{P_V(t)} + (A_V - A_2) \overline{P_C(t)} \quad (3)$$

$$\overline{\dot{m}_V(t)h_{tV}(t)} = \dot{m}_0 h_{t2} \quad (4)$$

Based on our numerical simulations of the filling process, we model the properties at the valve plane as piecewise constant functions of time. The velocity $u_V(t)$ and mass flow rate $\dot{m}_V(t)$ are equal to zero when the valve is closed and take on values u_V^o and \dot{m}_V^o when the valve is open, as illustrated in Fig. 5. Assuming

that the volume of the plenum is much larger than the volume of the detonation tube, the pressure inside the plenum can be approximated as constant. The pressure at the valve plane is equal to the average pressure in the cavity $\overline{P_C}$ when the valve is closed and takes a value P_V^o when the valve is open (Fig. 5). Rewriting the averaged energy equation in terms of the temperature, we obtain $T_{tV}^o = T_{t2}$. The average conditions in the plenum can be determined with the additional consideration of the flow in the detonation tube when the valve is open. In our present geometry, in which the valve plane corresponds to a geometrical throat, two different cases must be distinguished: either the flow at the valve plane is subsonic or it is sonic (choked).

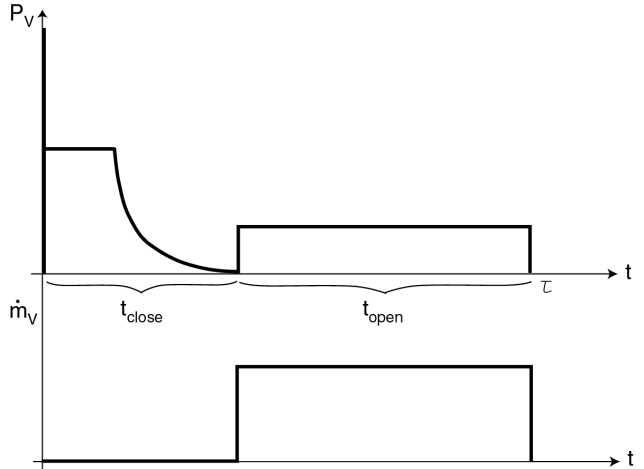


Fig. 5 Modeling of pressure and flow velocity at the valve plane during a cycle.

Subsonic flow at the valve plane

The unsteady expansion wave generated at valve opening propagates upstream in the plenum and sets up a steady expansion through the area change before decaying, becoming very weak for large area ratios. Assuming a large area ratio between the plenum and the valve, we ignore the weak unsteady expansion propagating in the plenum in our calculations. We model the flow during the filling process in the subsonic case by a steady expansion through the area contraction between the plenum and the detonation tube, and a shock wave propagating in the tube followed by the burned gases/fresh air contact surface, as shown in Fig. 6. We neglect the influence of the starting transient by assuming that the time necessary to start the steady flow is much smaller than the time necessary to fill the detonation tube. The interaction of the shock wave with the open end and any subsequent reflected waves are ignored. These assumptions are discussed with respect to the results of numerical simulations in the next section.

Since the expansion wave is steady, the total temperature is constant across it and we can estimate the average temperature in the plenum: $\overline{T_C} \approx \overline{T_{tC}} =$

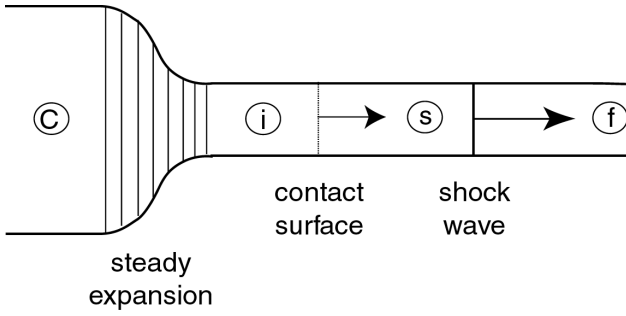


Fig. 6 Flow configuration used to model the filling process in the case of subsonic flow at the valve plane.

$\overline{T}_{tV} = T_{t2}$. Hence the average temperature inside the plenum is equal to the total temperature downstream of the inlet.

The conditions at the valve plane are determined from the average plenum conditions as a function of the velocity u_V , using the isentropic flow relationships through a steady expansion wave.

$$\overline{P}_C = P_{t2} - \frac{\dot{m}_0 u_V^o}{A_2} + \frac{\dot{m}_0 R \overline{T}_C}{A_2 u_V^o} \left(1 - \frac{u_V^{o2}}{2C_P \overline{T}_C} \right)^{-\frac{1}{\gamma-1}} \left[1 - \left(1 - \frac{u_V^{o2}}{2C_P \overline{T}_C} \right)^{\frac{\gamma}{\gamma-1}} \right] \quad (5)$$

The velocity at the valve plane is determined by matching the flow in the plenum with the downstream conditions in the detonation tube. The pressure ratio across the valve at opening determines the shock wave Mach number and the velocity at the valve plane, which is also the velocity of the contact surface. Matching conditions at the interface yields¹⁹

$$\overline{P}_C = P_0 \frac{1 + \frac{2\gamma_b}{\gamma_b+1}(M_S^2 - 1)}{\left[1 - \frac{2(\gamma-1)}{(\gamma_b+1)^2} \left(\frac{c_f}{c_C} \right)^2 (M_S - 1/M_S)^2 \right]^{\frac{\gamma_b}{\gamma_b-1}}} \quad (6)$$

The velocity at the valve plane is equal to the post-shock velocity in the burned gases

$$\frac{u_V^o}{c_f} = \frac{2}{\gamma_b + 1} \left(M_S - \frac{1}{M_S} \right) \quad (7)$$

We solve for M_S by equating Eqs. 5 and 6 and replacing u_V by the expression of Eq. 7 in Eq. 5. Once M_S is known, all the other variables of the system are calculated using the relationships across the shock and the expansion wave.

Choked flow at the valve plane

When the pressure ratio across the valve exceeds a critical value (given by $\overline{P}_C/P_V = ((\gamma+1)/2)^{\frac{\gamma}{\gamma-1}}$), the velocity at the valve plane, which is also the throat in our case, becomes sonic and the flow is choked.

The flow inside the plenum is then independent of the downstream conditions and it can be decoupled from the flow in the detonation tube, making the system easier to solve. The flow configuration is shown in Fig. 7. The velocity at the valve plane is equal to the speed of sound $u_V^o = c^*$. Using the relationships for choked flow at the valve plane, it is possible to directly estimate the average plenum pressure from Eq. 3:

$$\overline{P}_C = P_{t2} - \frac{\dot{m}_0 c^*}{\gamma A_2} \left[\gamma + 1 - \left(\frac{\gamma+1}{2} \right)^{\frac{\gamma}{\gamma-1}} \right] \quad (8)$$

The properties at the valve plane are given by the standard isentropic relations and the sonic condition.

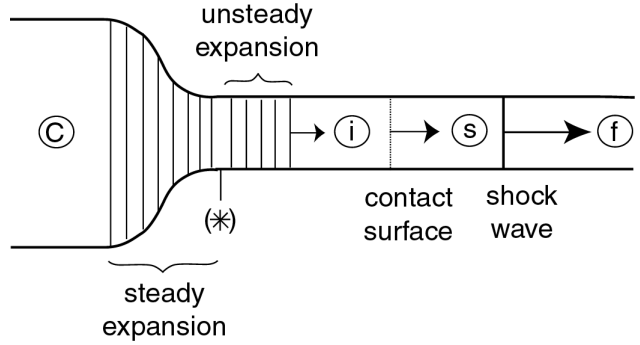


Fig. 7 Flow configuration used to model the filling process in the case of choked flow at the valve plane.

The flow in the detonation tube is calculated from a pressure-velocity diagram by matching conditions across the interface and solving for the shock wave Mach number¹⁹

$$\frac{\overline{P}_C}{P_0} = \frac{1 + \frac{2\gamma_b}{\gamma_b+1}(M_S^2 - 1)}{\left[\sqrt{\frac{\gamma+1}{2}} - \frac{\gamma-1}{\gamma_b+1} \frac{c_f}{c_C} (M_S - 1/M_S) \right]^{\frac{2\gamma}{\gamma-1}}} \quad (9)$$

Discussion

The coupling of the flow in the plenum with the flow in the detonation tube results in average conditions in the plenum that are different from the stagnation conditions downstream of the inlet. Although the average stagnation temperature in the plenum is equal to the stagnation temperature downstream of the inlet, the average plenum pressure is lower than the inlet stagnation pressure due to the unsteadiness of the flow in the plenum. The entropy increase associated with the unsteady waves due to valve opening and closing results in losses compared to the ideal steady flow case, for which total pressure is conserved. The ratio of the average plenum pressure to the stagnation pressure downstream of the inlet is shown as a function of the flight Mach number in Fig. 8. Values are given only for $M_0 \geq 1$ because we made the assumption of choked flow in the diffuser and constant inflow in the plenum. In the case considered in Fig. 8, \overline{P}_C is only 2.6% lower

than P_{t2} in the worst case. However, this value can become significant (greater than 10%) if the ratio of the plenum area to the inlet capture area A_2/A_0 is decreased.

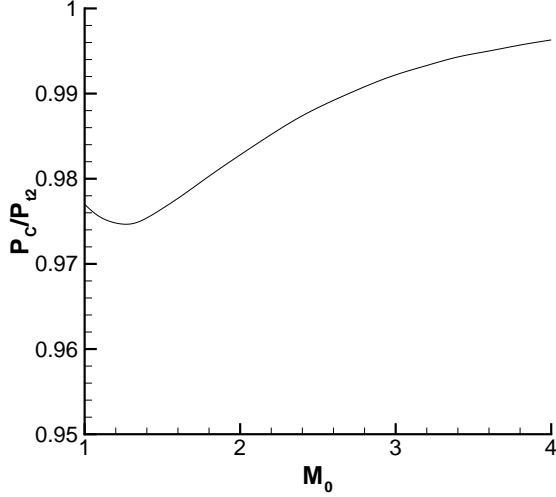


Fig. 8 Ratio of the average pressure in the plenum to the total pressure downstream of the inlet as a function of the flight Mach number. $P_0 = 0.265$ bar, $T_0 = 223$ K, $A_0 = 0.004$ m², $A_2 = 0.04$ m², $A_V = 0.006$ m².

In our calculations, we assumed fixed valve area A_V and valve close time; other parameters such as valve open time and detonation tube length are then determined by the periodicity of the system. This means that the open time was set as a free parameter determined by the average mass flow rate at the valve plane from the mass conservation equation: $\tau \dot{m}_0 = t_{open} \dot{m}_V^o$. This makes sense only if $\dot{m}_V^o > \dot{m}_0$. There is a critical value of the flight Mach number at which \dot{m}_V^o is exceeded by \dot{m}_0 , corresponding to an infinite open time. This critical value depends on the ratio of the valve area to the inlet capture area, and increases with decreasing A_V/A_0 . For realistic values of this parameter, this behavior is observed at subsonic flight conditions, at which the inlet flow would be strongly affected by the unsteady flow in the plenum, making our model inappropriate. In practice, when \dot{m}_V^o approaches \dot{m}_0 , the system will adjust itself to these conditions by sending pressure waves upstream in order to modify the inlet flow and to decrease the inlet mass flow rate, keeping the open time finite.

Comparison with numerical simulations

The predictions of our modeling for the filling process were compared with the results of the numerical simulations with Amrita¹⁸ described previously. An average velocity u_V and pressure P_V at the valve plane were calculated from the two-dimensional simulations by spatially and temporally averaging these quantities along the valve plane. An average filling velocity U_{fill}

was calculated as the average velocity of the inlet air-burned gases contact surface between the valve plane and the tube exit. Fig. 9 shows these quantities as a function of the initial pressure ratio P_R for both model and simulations.

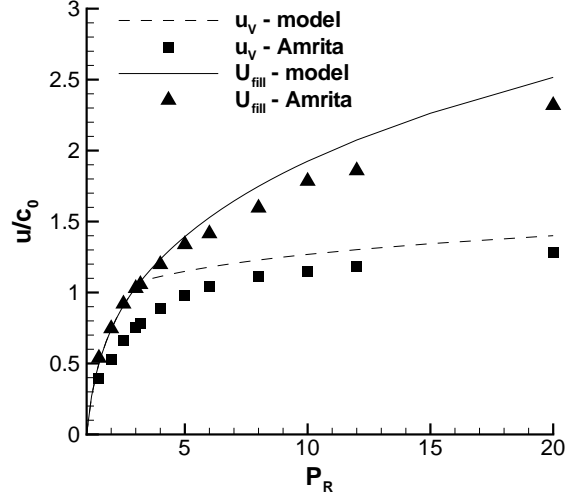


Fig. 9 Comparison of model predictions and numerical simulations with Amrita¹⁸ for the velocity at the valve plane and the average filling velocity. $T_f/T_0 = 7.69$, $\gamma = 1.4$.

According to our one-dimensional model, the flow at the valve plane is expected to become choked above a critical value of the pressure ratio equal to 3.19 in the case considered. For pressure ratios below this value, $u_V = U_{fill}$. For higher values of P_R , the flow is choked at the valve plane and an unsteady expansion accelerates the flow to supersonic downstream of the valve plane, so that $u_V \neq U_{fill}$. The velocity at the valve plane is predicted by the speed of sound at the throat c^* , while the filling velocity is predicted by the velocity of the flow behind the shock wave. The two curves in Fig. 9 correspond to these two cases.

The model predictions for U_{fill} are in reasonable agreement with the results of the numerical simulations, with a maximum deviation of 11%, respectively. The model predictions for u_V are systematically higher than the numerical results by up to 40% near choking. The discrepancies in the velocity at the valve plane can be attributed to the influence of the starting transient, which is ignored by our model but is characterized by a lower flow velocity than in the steady expansion case, and to the effect of two-dimensional waves generated at valve opening, which strongly affect the flow at the valve plane. The influence of the reflected waves generated at the open end was investigated by conducting simulations with an infinitely long tube but the difference observed was minimal.

The values of the flow properties at the end of the filling process are critical to the calculation of the deto-

nation tube impulse. The model assumes that the flow in the detonation tube is uniform and moving at a velocity U_{fill} and at a pressure equal to the post-shock pressure. In order to test the validity of this approximation, we plotted the pressure and velocity profile along the centerline from our numerical simulations in Fig. 10. The pressure profile indicates that the flow inside the detonation tube is relatively uniform in the first half of the tube but quite non-uniform in the second half, where it includes a quasi-steady left-facing shock followed by a steady expansion near the open end. The spatially averaged model pressure at the end of the filling process is between 5.8% and 22.7% higher than the average pressure in the tube from the numerical simulations for values of P_R between 2 and 10. These numbers are helpful to understand the influence of our approximations on the accuracy of our predictions and their potential consequence on performance parameters.

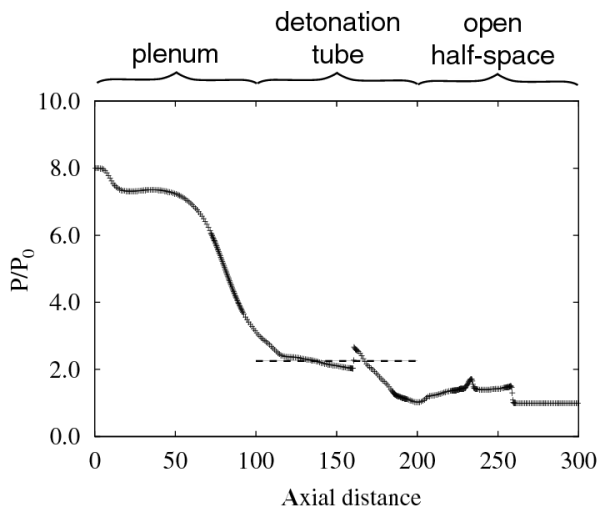


Fig. 10 Pressure profile along the centerline from the numerical simulations with Amrita.¹⁸ The valve is located at an axial distance of 100 and the detonation tube exit is located at 200. The dashed line shows the value of the model prediction. $P_R = 8$, $T_f/T_0 = 7.69$, $\gamma = 1.4$.

Flow in the plenum

The unsteady pressure waves generated by valve closing and opening strongly affect the overall flow in the plenum, which, in turn, influences the flow through the inlet diffuser. Since conventional steady inlets may be sensitive to downstream pressure fluctuations, it is critical to be able to model the unsteady flow in the plenum.

We assume that the cycle time is much larger than the characteristic acoustic time in the plenum, so that the properties in the plenum can be modeled as spatially uniform. We assume that the incoming flow is choked at the diffuser. The flow downstream of the inlet diffuser has a low Mach number, so that the flow

velocity in the cavity is small and we can neglect the kinetic energy term when calculating the total energy and the total enthalpy. We model the flow into the detonation tube with a steady expansion so that the total enthalpy is conserved between the cavity and the valve plane. In order to model the unsteady flow in the plenum, we solve the unsteady mass and energy equations for the control volume V_C (Fig. 4).

$$V_C \frac{d\rho_C}{dt} = \dot{m}_0 - \dot{m}_V(t) \quad (10)$$

$$V_C \rho_C(t) \frac{dT_C}{dt} = \gamma \dot{m}_0 T_{t2} - [\dot{m}_0 + (\gamma - 1)\dot{m}_V(t)] T_C(t) \quad (11)$$

This system of equations has to be solved separately for the closed part of the cycle $[0, t_{close}]$ and for the open part of the cycle $[t_{close}, \tau]$. Assuming small variations in the properties inside the plenum and because the flow in the detonation tube during the open part of the cycle is generated by a steady expansion, we approximate $\dot{m}_V(t)$ as constant during the open part of the cycle, as in the previous section. For sufficiently large supersonic flight Mach numbers, the flow at the valve plane during the filling process is choked, and this approximation is justified. We are seeking the limit cycle solution to this system of equations, which corresponds to periodic behavior.

The density varies linearly around its average value $\overline{\rho_C}$. The limit cycle solution for the temperature has to obey the averaged energy equation, which states that the average temperature during the open part of the cycle is equal to T_{t2} . The solution for the temperature evolution was obtained numerically and is shown in Fig. 11. The numerical solution quickly converges towards the limit cycle. After 10 cycles, the average value of the temperature in the plenum during a cycle was found to be within 0.35% of $\overline{T_C}$. This means that our averaged conservation equations for the plenum are consistent with the unsteady analysis of the flow in the plenum. The characteristic acoustic time in this case was estimated as $V_C^{1/3}/\overline{c_C}$ and verified to be much lower than t_{close} .

The amplitude of the fluctuations in density and temperature in the cavity can be determined analytically:

$$\frac{\Delta\rho_C}{\overline{\rho_C}} = \frac{\dot{m}_0 t_{close}}{2V_C \overline{\rho_C}} \quad (12)$$

The amplitude of fluctuations in density, temperature, and pressure for the case shown in Fig. 11 are 15.2%, 6.1%, and 22.1%, respectively. The amplitude of the fluctuations are all controlled by the same non-dimensional parameter $\dot{m}_0 t_{close}/(V_C \overline{\rho_C})$, which represents the ratio of the amount of mass added to the system during the closed part of the cycle to the average mass in the plenum. The amplitude of oscillations is reduced for a lower mass flow rate (corresponding to a lower flight Mach number), a lower close time,

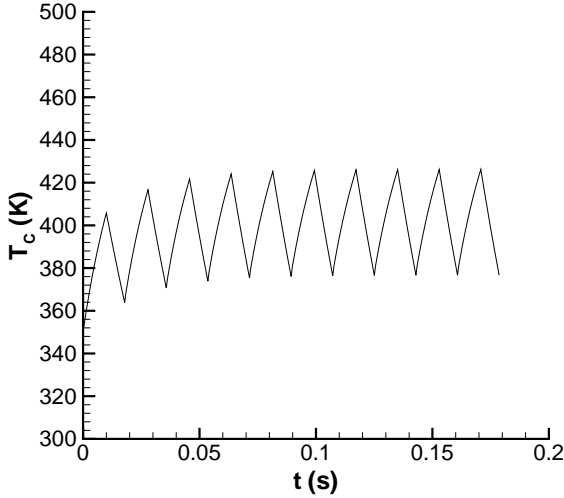


Fig. 11 Evolution of temperature in the plenum. $A_0 = 0.004 \text{ m}^2$, $A_2 = 0.04 \text{ m}^2$, $A_V = 0.006 \text{ m}^2$, $V_C = 0.02 \text{ m}^3$, $\dot{m}_0 = 0.9915 \text{ kg/s}$, $\overline{P_C} = 1.885 \text{ bar}$, $\overline{T_C} = 401.4 \text{ K}$, $t_{close} = 0.01 \text{ s}$, $t_{open} = 0.007865 \text{ s}$.

a higher plenum volume, or a higher average plenum density.

The pressure oscillations in the cavity induce an unsteady behavior of the flow in the inlet diffuser. This behavior has been previously studied in the context of longitudinal pressure fluctuations generated by combustion instabilities in ramjets. The effect of pressure oscillations on the inlet may be regarded as an equivalent loss of pressure margin that might result in inlet unstart. Higher frequency oscillations tend to stabilize the diffuser shock.^{20–22} The frequency of oscillations in the cavity is given by $1/\tau$, which means that reducing the cycle time is going to benefit inlet stability. For a given inlet configuration and flight condition, the amplitude of the pressure oscillations in the cavity decreases with decreasing close time and increasing plenum volume. This analysis gives some general ideas about the unsteady response of the inlet diffuser.

Control volume analysis

The performance of an air-breathing PDE is determined by performing an unsteady open-system control volume analysis. The control volume Ω considered, displayed in Fig. 12, is stationary with respect to the engine. The engine is attached to the vehicle through a structural support. The control surface Σ passes through the engine valve plane, encompasses the detonation tube, and extends far upstream of the inlet plane. The side surfaces are parallel to the freestream velocity. We consider the equations for mass, energy, and momentum for this control volume.

Mass conservation

Writing the general unsteady conservation equation for mass in the control volume Ω , bounded by the sur-

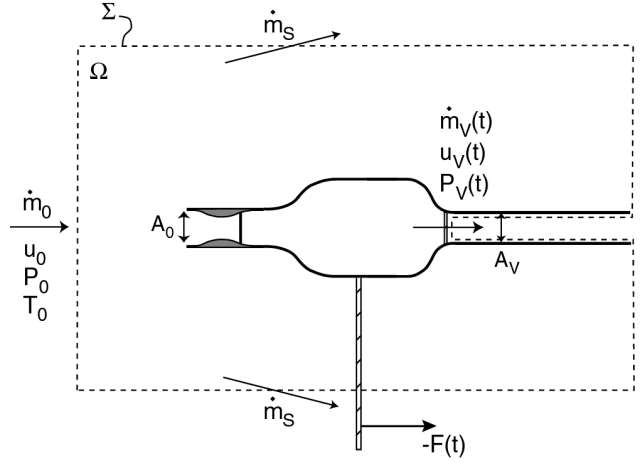


Fig. 12 Control volume considered for analysis of single-tube PDE.

face Σ :

$$\frac{d\mathcal{M}}{dt} + \dot{m}_V(t) - \rho_0 u_0 A_V + \dot{m}_s = 0 \quad (13)$$

Since there is no average mass storage inside the engine, we can integrate over a cycle the mass conservation equation between the inlet plane and the valve plane:

$$\int_0^\tau \dot{m}_V(t) dt = \tau \dot{m}_0 \quad (14)$$

This result can be used when integrating the mass conservation equation for the control volume Ω over a cycle. With the assumption of no mass storage in the engine through a cycle during steady flight, we can calculate the mass flow of air through the side surfaces of Ω :

$$\dot{m}_s = \rho_0 u_0 (A_V - A_0) \quad (15)$$

Momentum conservation

The forces on the control volume consist of the pressure forces and the reaction to the thrust carried through the structural support. If we assume that the sides of the control volume are sufficiently distant from the engine, then the flow crosses the side control surface with an essentially undisturbed velocity component in the flight direction. Applying the momentum equation in the flight direction, and using the result of Eq. 15, we obtain an expression for the instantaneous thrust:²³

$$F(t) = \dot{m}_V(t) u_V(t) - \dot{m}_0 u_0 + A_V (P_V(t) - P_0) + \frac{d}{dt} \int_{\Omega} \rho u dV \quad (16)$$

The last term represents the unsteady variation of momentum inside the control volume.

Energy conservation

The general unsteady conservation equation for energy in the control volume Ω is, in the absence of body

forces or heat release in the control volume (heat is released only in the detonation tube, which is outside our control volume Ω):

$$\frac{d}{dt} \int_{\Omega} \rho(e + u^2/2) dV + \dot{m}_V(t) h_{tV}(t) - \dot{m}_0 h_{t0} = 0 \quad (17)$$

after using the result of Eq. 15. Integrating over a cycle, the first term vanishes because there is no average energy storage in the control volume. Using Eq. 14, the energy equation results in: $h_{tV}^o = h_{t0}$. It states that the stagnation enthalpy of the flow has to be conserved between the freestream and the valve plane during the open part of the cycle. This is satisfied by our model, since the stagnation enthalpy of the plenum is equal to the freestream stagnation enthalpy, and the flow into the detonation tube during the open part is generated by a steady expansion, which conserves stagnation enthalpy. The energy release in the detonation is implicitly considered in the calculation of the detonation tube impulse.

Thrust calculation

The average thrust is calculated by averaging Eq. 16 over a complete cycle. The unsteady term can be integrated and corresponds to the variation in total momentum in the control volume during a cycle, which vanishes during steady flight, since the total momentum in the control volume has a periodic behavior. During the closed part of the cycle (from 0 to t_{close}), the contribution of the momentum at the valve plane vanishes since the valve is closed. The pressure contribution corresponds to the conventional detonation tube impulse I_{dt} generated by the detonation and blowdown processes

$$\int_0^{t_{close}} A_V(P_V(t) - P_0) dt = I_{dt} \quad (18)$$

The momentum and pressure contributions of the detonation tube during the open part of the cycle (from t_{close} to τ) are calculated using the model estimates for velocity and pressure at the valve plane during the open part of the cycle. Using Eq. 14, the pressure and momentum contribution for the open part of the cycle is:

$$\int_{t_{close}}^{\tau} (\dot{m}_V(t) u_V(t) dt + A_V(P_V(t) - P_0)) dt = \tau \dot{m}_0 u_V^o + A_V(P_V^o - P_0) t_{open} \quad (19)$$

Using Eqs. 18 and 19, the average thrust can be expressed as follows

$$\bar{F} = \frac{1}{\tau} I_{dt} + \dot{m}_0 (u_V^o - u_0) + \frac{t_{open}}{\tau} A_V(P_V^o - P_0) \quad (20)$$

The average thrust of an air-breathing PDE is determined by the contributions of detonation tube impulse, ram momentum, and ram pressure in the engine.

Influence of the purging time

The purging time has a strong influence on the overall engine thrust since the thrust is inversely proportional to the cycle time, and, by definition, $\tau = t_{close} + t_{purge} + t_{fill}$. Since t_{open} is determined in our model by the condition for periodicity, increasing t_{purge} means decreasing t_{fill} and decreasing the mass of detonable gas in the detonation tube.

For a fixed open time, the purging time relates the incoming mass flow rate to the mixture mass detonated in the chamber. We assume that the detonation tube has a volume equal to the volume of the slug of combustible gas injected^a. Assuming ideal fuel-air mixing at constant pressure and temperature, the mass balance in the detonation tube shows that:

$$V = \left(\frac{1+f}{1+\pi} \right) \frac{\tau \dot{m}_0}{\rho_i} \quad (21)$$

where $\pi = t_{purge}/t_{fill}$ is defined as the purge coefficient. It is critical to make the distinction between the air mass flow rate \dot{m}_0 and the average detonated mixture mass flow rate $\rho_i V/\tau$. The average fuel mass flow rate is given by:

$$\dot{m}_f = \frac{\rho_i V f}{(1+f)\tau} \quad (22)$$

The fuel-based specific impulse is calculated with respect to the fuel mass flow rate as

$$\begin{aligned} I_{SPF} &= \frac{\bar{F}}{\dot{m}_f g} \\ &= I_{SPFdt} + \frac{1+\pi}{fg} \left[u_V^o - u_0 + \frac{A_V(P_V^o - P_0)}{\dot{m}_V^o} \right] \end{aligned} \quad (23)$$

The fuel-based specific impulse is the sum of three terms representing the contributions of the detonation process, the ram momentum, and the ram pressure in the engine. The first term is always positive. The second term is negative because of the flow losses associated with decelerating the flow through the inlet and re-accelerating it unsteadily during the filling process. The third term is positive because the air injected during the filling process is at higher pressure than the outside air. However, the sum of the last two terms is negative and corresponds to a drag term due to flow losses and unsteadiness. The specific impulse decreases linearly with increasing purge coefficient.

Detonation tube impulse

The static impulse of a PDE is due to the detonation process (first term on right-hand side of Eq. 23) and has been measured¹⁻⁵ for single-cycle operation and

^aThis means the length of the detonation tube is being varied with the operating conditions in this model.

several models have been proposed.^{3,6,7} However, in practice, the flow downstream of the detonation wave in a moving engine is not going to be at rest because of the filling process. This is captured in multi-cycle experiments^{3,10} but the values obtained for the impulse are still well predicted by the single-cycle estimates⁷ because the filling occurs at low subsonic velocity in these tests. During supersonic flight, the large pressure ratio across the valve will generate high filling velocities during the filling process, which can significantly alter the flow field and the detonation/blowdown process. We need to include this effect in our model. In an idealized case, we assume that the detonation wave is initiated immediately after valve closing. The detonation wave catches up with the expansion wave generated by the valve closing and the situation before the wave exits the tube corresponds to a detonation wave propagating in a flow moving in the same direction at the filling velocity.

The detonation wave is followed by an expansion wave, referred to as the Taylor wave, which brings the products back to rest near the closed end of the tube. In the moving flow case, the energy release across the wave is identical to the no flow case and the CJ pressure, temperature, density, and speed of sound are unchanged. However, the wave is now moving at a velocity $U_{CJ} + U_{fill}$ with respect to the tube. The properties upstream of the Taylor wave, near the closed end, are modified compared to the no flow case because the flow behind the detonation wave has to undergo a stronger expansion. Using the method of characteristics as described in Wintenberger et al.,⁷ we can obtain the speed of sound and the pressure behind the Taylor wave:

$$c_3 = \frac{\gamma_b + 1}{2} c_{CJ} - \frac{\gamma_b - 1}{2} (U_{CJ} + U_{fill}) \quad (24)$$

$$P_3 = P_{CJ} \left(\frac{c_3}{c_{CJ}} \right)^{\frac{2\gamma_b}{\gamma_b - 1}} \quad (25)$$

The pressure behind the Taylor wave decreases as the filling velocity increases due to the additional expansion required to bring the flow to rest at the wall. The Taylor wave also occupies a larger region of the tube behind the detonation in the moving flow case.

The detonation tube impulse is calculated as the integral of the pressure trace at the valve plane (or thrust wall):

$$I_{dt} = \int_0^{t_{close}} A_V (P_3(t) - P_0) dt \quad (26)$$

Using dimensional analysis, we idealize the pressure trace at the thrust wall and model the pressure trace integral in a similar fashion as described in Wintenberger et al.⁷ The pressure history is modeled by a constant pressure region followed by a decay due to

gas expansion out of the tube. The detonation tube impulse can then be expressed as:

$$\int_{t_{open}}^{\tau} (P_3(t) - P_0) dt = \Delta P_3 \left[\frac{L}{U_{CJ} + U_{fill}} + (\alpha + \beta) \frac{L}{c_3} \right] \quad (27)$$

where $\Delta P_3 = P_3 - P_0$, α is a non-dimensional parameter corresponding to the time taken by the first reflected characteristic at the open end to reach the thrust wall, and β is a non-dimensional parameter corresponding to the pressure decay period.⁷ The first part of the term in square brackets in Eq. 27 is equal to the time taken by the detonation wave to propagate to the open end. As in the no flow case, it is possible to derive a similarity solution for the reflection of the first characteristic at the open end and to analytically calculate α . The reader is referred to Wintenberger et al.⁷ for the details of the derivation in the no flow case. For the moving flow case, the value of α is:

$$\alpha = \frac{c_3}{U_{CJ} + U_{fill}} \cdot \left[2 \left(\frac{\gamma_b - 1}{\gamma_b + 1} \left(\frac{c_3 - u_{CJ}}{c_{CJ}} + \frac{2}{\gamma_b - 1} \right) \right)^{-\frac{\gamma_b + 1}{2(\gamma_b - 1)}} - 1 \right] \quad (28)$$

The value of β was assumed to be independent of the filling velocity and the same value as in Wintenberger et al.⁷ was used: $\beta = 0.53$.

In order to validate the model for the thrust wall pressure integration (Eq. 27), the flow was simulated numerically using Amrita.¹⁸ The simulation solved the non-reactive Euler equations using a Kappa-MUSCL-HLLE solver in the two-dimensional (cylindrical symmetry) computational domain consisting of a straight tube of length L closed at the left end and open to a half-space at the right end. The moving flow was represented by an idealized inviscid straight pressure-matched jet profile at constant velocity U_{fill} as shown on Fig. 13. The modified Taylor wave similarity solution was used as an initial condition, assuming the detonation has just reached the open end of the tube when the simulation is started. This solution was calculated using a one- γ model for detonations²⁴ for a non-dimensional energy release $q/RT_i = 40$ across the detonation and $\gamma = 1.2$ for reactants and products. The corresponding CJ parameters are $M_{CJ} = 5.6$ and $P_{CJ}/P_i = 17.5$, values representative of stoichiometric hydrocarbon-air mixtures. The initial refilling pressure P_i ahead of the detonation wave was taken to be equal to the pressure P_0 outside the detonation tube. The configuration adopted for the moving flow is a very elementary representation of the flow at the end of the filling process, which will, in reality, include vortices associated with the unsteady flow and the unstable jet shear layers. However, the analysis of the numerical simulations showed that the flow in the tube is

one-dimensional except for within one to two tube diameters from the open end and mainly dictated by the gas dynamic processes at the tube exit plane. Since the exit flow is choked for most of the process, the influence of our simplified jet profile on the process, the influence of our simplified jet profile on the thrust wall pressure integration is minimal. Fig. 14 shows the comparison of the non-dimensionalized thrust wall pressure integral as a function of the filling Mach number with the predictions of our model. The numerical pressure integration was carried out for a time equal to $20t_{CJ}$. As the filling Mach number increases, the flow expansion through the Taylor wave is more severe and the plateau pressure behind the Taylor wave P_3 decreases. Even though P_3 is lower, the blowdown process is accelerated due to the presence of the initial moving flow. The overall result is that the detonation tube impulse decreases with increasing filling Mach number, as shown in Fig. 14, mainly due to the stronger expansion through the Taylor wave as M_{fill} increases. The model agrees reasonably well with the results of the numerical simulations. It generally overpredicts the results of the numerical simulations by as much as 25% at higher filling Mach numbers. The agreement is better at lower Mach numbers (within 11% error for $M_{fill} \leq 2$ and 4% for $M_{fill} \leq 1$).

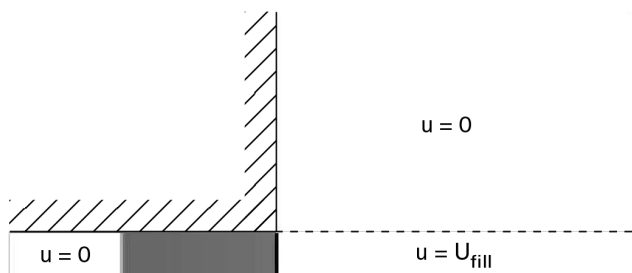


Fig. 13 Numerical Schlieren image of the initial configuration for the numerical simulations of the detonation process with moving flow. The Taylor wave is visible behind the detonation front at the tube exit.

Performance calculations

Performance calculations are carried out for a single-tube air-breathing PDE at sea level for hydrogen and JP10 fuels.

Model input parameters

The input parameters for the performance model described in Eq. 23 consist of the engine geometry, the freestream pressure and temperature, the flight Mach number, the specific heat ratio of air, the fuel type and stoichiometry, the valve close time, and the purging time.

The total pressure loss across the inlet during supersonic flight is modeled using the military specification MIL-E-5008B,²⁵ which specifies the total pressure ratio across the inlet as a function of the flight Mach

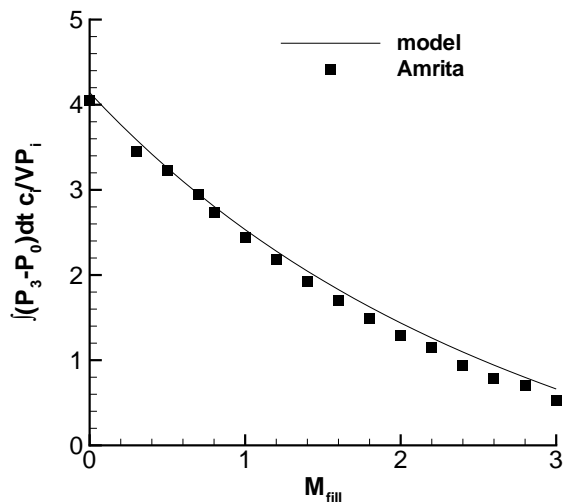


Fig. 14 Non-dimensional detonation tube impulse as a function of the filling Mach number. Comparison of model predictions based on Eq. 27 and results of numerical simulations with Amrita.¹⁸

number, for $M_0 > 1$:

$$\frac{P_{t2}}{P_{t0}} = 1 - 0.075(M_0 - 1)^{1.35} \quad (29)$$

The calculations of the initial conditions for the detonation require solving Eqs. 5 and 6 or 8 and 9, which require the knowledge of the specific heat ratio γ_b and the speed of sound c_f in the burned gases at the end of the blowdown. γ_b and the CJ parameters are obtained by carrying out detonation equilibrium computations using realistic thermochemistry.²⁶ The speed of sound c_f is calculated assuming that the flow is isentropically expanded from the CJ pressure to atmospheric pressure. This entire process needs to be iterated since the CJ parameters are obtained from P_i and T_i , which are determined from M_S , which is itself a function of γ_b and c_f . The solution was found by iteration until the prescribed values of γ_b and c_f matched the values obtained at the end of the equilibrium computations.

We estimate performance for an idealized configuration with the detonation tube completely filled with reactants before detonation initiation. Since the filling conditions, in particular the filling velocity and the fill time, vary with flight conditions, the length and volume of the detonation tube are also varied (Eq. 21).

Conditions inside the engine

The calculation of performance parameters first requires solving for the conditions inside the engine, in particular those in the plenum and the filling conditions in the detonation tube, including the filling velocity, which determines the cycle frequency. Fig. 15 shows the filling velocity and the velocity at the valve plane for a PDE operating with stoichiometric hydrogen-air flying at an altitude of 10,000 m. In this

particular case, the flow at the valve plane is predicted to remain subsonic up to a flight Mach number of 1.36, above which it becomes choked. For $M_0 > 1.36$, U_{fill} exceeds u_V because of the additional unsteady expansion generated at the valve plane. The filling velocity increases with increasing flight Mach number because of the increased stagnation pressure in the plenum, which generates a stronger shock wave at valve opening.

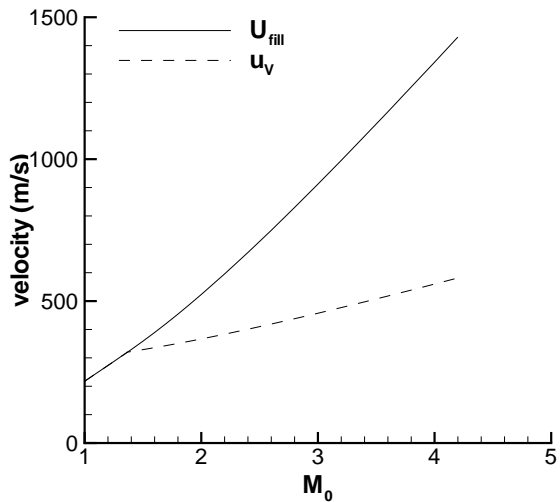


Fig. 15 Filling velocity and velocity at the valve plane as a function of flight Mach number for single-tube PDE operating with stoichiometric hydrogen-air. $Z = 10,000$ m, $A_0 = 0.004$ m², $A_2 = 0.04$ m², $A_V = 0.006$ m², $t_{close} = 0.005$ s.

Fig. 16 shows the pressure non-dimensionalized with the freestream stagnation pressure at various locations inside the engine. The inlet stagnation pressure decreases with increasing flight Mach number relative to the freestream stagnation pressure due to the stagnation pressure losses across a supersonic inlet (Eq. 29). The average plenum pressure is slightly lower than P_{t2} (see Fig. 8). The pressure at the valve plane is equal to the filling pressure until the valve plane becomes choked. At higher values of M_0 , the additional unsteady expansion lowers even further the filling pressure compared to the freestream total pressure. An important point is that, even though the average plenum pressure strongly increases with flight Mach number, the ratio of the filling pressure to the freestream total pressure decreases sharply, due to the substantial values obtained for the filling velocity (see Fig. 15).

PDE performance parameters

Variation with flight Mach number

Performance parameters are calculated for an air-breathing PDE operating with stoichiometric hydrogen-air and JP10-air. The specific impulse is shown in Fig. 17 as a function of the flight Mach num-

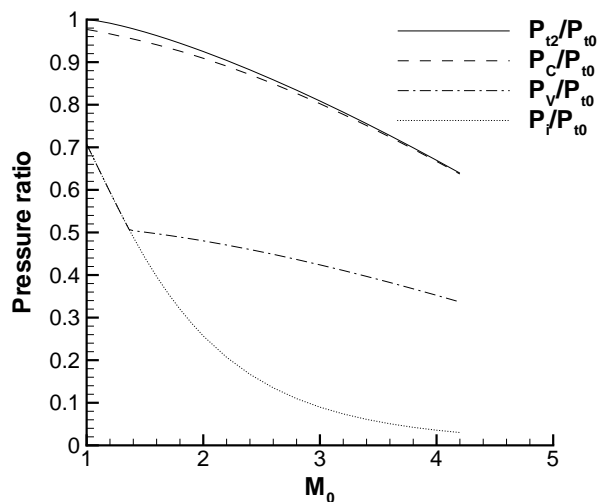


Fig. 16 Inlet stagnation pressure, plenum pressure, pressure at the valve plane, and filling pressure non-dimensionalized with freestream total pressure as a function of flight Mach number. Stoichiometric hydrogen-air, $Z = 10,000$ m, $A_0 = 0.004$ m², $A_2 = 0.04$ m², $A_V = 0.006$ m².

ber for conditions at 10,000 m altitude. The results shown in Fig. 17 represent the maximum values predicted by the model for a given engine geometry (no purging). We restrict ourselves to performance calculations for supersonic flight because of the assumptions made in the derivation of the model. A data point from the static multi-cycle experiments of Schauer et al.¹⁰ is given as a reference point for hydrogen in the static case. A data point for a ballistic pendulum experiment²⁷ for stoichiometric JP10-air at 100 kPa and 330 K is given as a reference for the static case. Single-cycle static impulse predictions⁷ are also shown for conditions corresponding to an altitude of 10,000 m for both hydrogen and JP10. Even though the present model assumptions do not apply for subsonic flight, the reference values for the static case ($M_0 = 0$) apparently lie on or close to a linear extrapolation of the results obtained for supersonic flight. Our single-tube PDE generates thrust up to a flight Mach number of 4.2 for hydrogen and 4 for JP10.

The specific impulse decreases almost linearly with increasing flight Mach number from a value at $M_0 = 1$ of about 3530 s for hydrogen and 1370 s for JP10. The detonation tube impulse decreases with increasing flight Mach number due to the increasing filling velocity (see Fig. 15), as observed previously (Fig. 14). For choked flow at the valve plane, the ram momentum term decreases linearly with M_0 . If we neglect the outside pressure P_0 , the ram pressure term is proportional to $\sqrt{T_{t0}}$, and, therefore, increases with M_0 . However, as pointed out before, the sum of these two terms is negative and corresponds to a drag term increasing with increasing flight Mach number, caused by the

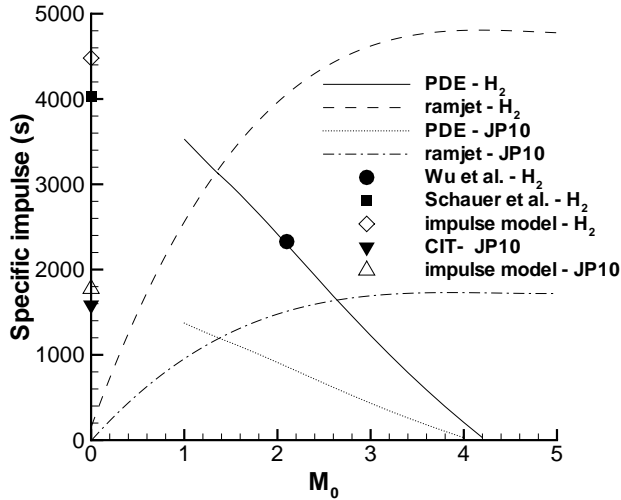


Fig. 17 Specific impulse of a single-tube air-breathing PDE compared to the ramjet operating with stoichiometric hydrogen-air and JP10-air. $Z = 10,000$ m, $A_0 = 0.004$ m², $A_2 = 0.04$ m², $A_V = 0.006$ m², $\pi = 0$. Data from multi-cycle numerical simulations¹² by Wu et al. for $M_0 = 2.1$ at 9,300 m altitude are shown. Experimental data from Schauer et al.¹⁰ and Caltech²⁷ and impulse model predictions⁷ are also given as a reference for the static case.

stagnation pressure loss through the inlet (Eq. 29).

Fig. 17 also shows a data point from the numerical simulations by Wu et al.,¹² who calculated the performance of an air-breathing PDE with a straight detonation tube flying at $M_0 = 2.1$ at an altitude of 9.3 km and operating with stoichiometric hydrogen-air. The model prediction at the same conditions, 2286 s, is within 1.8% of their baseline case (2328 s¹²).

Variation with altitude

Calculations show that the specific impulse decreases with decreasing altitude. For example, the specific impulse at sea level is systematically lower than that at 10,000 m by 150-300 s. It is possible to show using scaling arguments that the different components of the engine specific impulse are all independent of pressure, but vary with outside temperature. Increasing T_0 results in a stronger shock wave at valve opening, and, therefore, in a higher filling velocity, which results in a decrease in detonation tube specific impulse. The decrease in I_{SPFdt} is the main contribution to the decrease in engine specific impulse with decreasing altitude.

Variation with purge coefficient

As shown earlier (Eq. 23), the effect of purging is to decrease the specific impulse of the PDE. Increasing the purge coefficient results in an increase of the drag term in the specific impulse equation and, therefore, in a decrease of the overall specific impulse. At given

flight conditions, the specific impulse decreases linearly with increasing purge coefficient. Fig. 18 shows that the reduction in performance due to an increase in purge coefficient increases with flight Mach number, because of the increasing size of the drag term at higher flight Mach numbers. The purge coefficient is found to have a substantial effect on the thrust-producing range of an air-breathing PDE. Fig. 18 shows that the maximum flight Mach number for a hydrogen-fueled PDE at an altitude of 10,000 m decreases from 4.2 at $\pi = 0$ to 3.8 at $\pi = 0.5$ and 3.5 at $\pi = 1$.

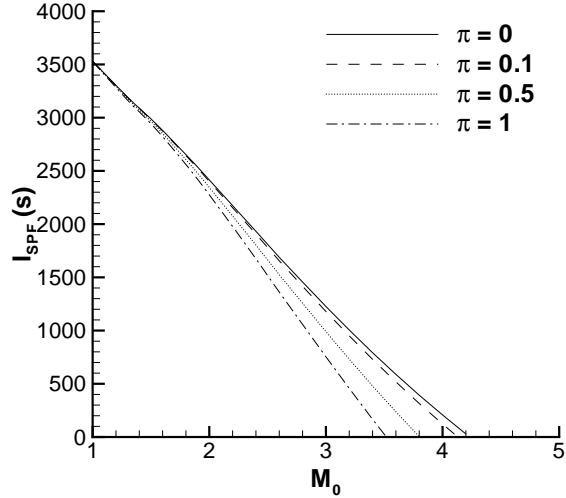


Fig. 18 Specific impulse of a single-tube PDE operating with stoichiometric hydrogen-air as a function of flight Mach number varying the purge coefficient. $Z = 10,000$ m, $A_0 = 0.004$ m², $A_2 = 0.04$ m², $A_V = 0.006$ m².

Issues associated with JP10

Recalculating the conditions inside the engine for JP10, it is found that the temperature of the flow at the valve plane exceeds the auto-ignition temperature of JP10-air (518 K²⁸) above $M_0 = 3$. This means that if the fuel injection system is located at the valve plane, pre-ignition of the JP10-air mixture is expected above Mach 3 before the detonation can be initiated, resulting in a significant decrease in detonation tube impulse due to potential expulsion of unburned reactants out of the detonation tube⁵ and reduction in thrust surface as part of the combustion process will take place while the valve is open. The filling temperature T_i remains below the auto-ignition temperature of JP10 across the entire range of flight Mach numbers.

Another issue with the use of liquid hydrocarbon fuels is related to potential condensation of the fuel in the detonation tube due to the low filling temperature. For the case considered here with JP10, the filling temperature remains under 300 K as long as $M_0 < 2.3$. The fuel injected will vaporize completely

as long as its vapor pressure is high enough at the temperature considered. It is possible that not all the fuel corresponding to stoichiometric quantity will be able to vaporize, and the engine may have to be run at a leaner composition depending on the flight conditions considered.

Comparison with conventional propulsion systems

The performance of a single-tube air-breathing PDE is compared with that of the ideal ramjet for flight conditions corresponding to 10,000 m altitude in Fig. 17. Performance was calculated for both engines for hydrogen and JP10, assuming they operate at stoichiometry. The ideal ramjet performance was calculated following the ideal Brayton cycle, taking into account the stagnation pressure loss across the inlet (taken equal to that undergone by the PDE), realistic thermochemistry,²⁶ and assuming thermodynamic equilibrium at every point in the nozzle. According to our performance predictions, the single-tube air-breathing PDE in the present configuration (straight detonation tube) has a higher specific impulse than the ideal ramjet for $M_0 < 1.35$ for both hydrogen and JP10 fuels.

The results of our performance calculations show that PDEs in the simple configuration considered (straight detonation tube) are not competitive with conventional steady propulsion systems at high supersonic flight Mach numbers, because of the increased total pressure loss across the inlet and the decreasing detonation tube impulse associated with the very high filling velocities and correspondingly low pressure and density in the detonation tube prior to detonation initiation. Adding a choked converging-diverging exit nozzle has been proposed by several researchers^{11,12} as a means to increase the chamber pressure and decrease the effective filling velocity of the detonation tube. The strong sensitivity of the detonation tube impulse to the filling velocity suggests a potential for improving performance, provided that the filling velocity can be decreased without excessive internal flow losses. The numerical simulations of Wu et al.¹² support this idea, showing an increase in specific impulse of up to 45% with the addition of a converging-diverging nozzle.

Uncertainty analysis

Since our performance model is based on many simplifying assumptions, we need to estimate the effect of the uncertainty on the performance parameters. Unfortunately, due to the complexity and the unsteadiness of the flow in a pulse detonation engine, which involves moving parts and chemical kinetics, there is no existing standard to which our model can be compared. It is difficult to estimate the influence of our assumptions unless a numerical simulation of the entire system is conducted. At present, only Wu et al.¹² and Ma et al.¹³ have published such computations and although our work agrees with their results at a single

condition, this is far from conclusive validation of our approach.

We know from our numerical simulations of the filling process the uncertainty of the model predictions of some of the parameters. We carried out best case and worst case scenario calculations to estimate the model uncertainty for a stoichiometric hydrogen-air PDE flying at 10,000 m with no purging. The result of these calculations is given in Fig. 19. The region of uncertainty is the grey shaded area around the predicted specific impulse curve. As expected, the uncertainty margin is quite large and increases with increasing flight Mach number, due to the growing uncertainty on the detonation tube impulse. The uncertainty on the specific impulse at $M_0 = 1$ is $\pm 9.9\%$ and at $M_0 = 2$, it is $-36.5\%/+12.7\%$. Since the predicted detonation tube impulse overpredicts the numerical values, the magnitude of the uncertainty in the worst case scenario is larger than that in the best case scenario.

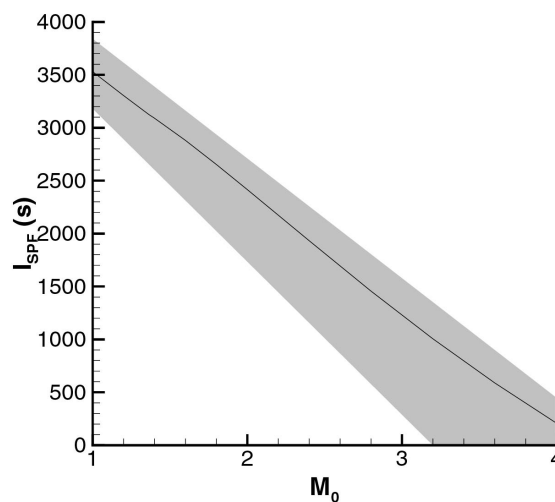


Fig. 19 Uncertainty associated with the calculation of specific impulse for a stoichiometric hydrogen-air PDE. The uncertainty region is the shaded area. $Z = 10,000$ m, $A_0 = 0.004$ m², $A_2 = 0.04$ m², $A_V = 0.006$ m², $\pi = 0$.

Conclusions

We have developed a simple model for predicting the performance of a single-tube air-breathing pulse detonation engine based on gas dynamics and control volume methods. The model offers the possibility to evaluate in a simple way the performance of a single-tube PDE consisting of a steady supersonic inlet, a large plenum, and a straight detonation tube. Numerical simulations showed that the filling process is characterized by a shock wave generated at valve opening and propagating in the detonation tube and a combination of unsteady and steady expansions between the plenum and the detonation tube. The flow in the plenum is coupled to the flow in the detonation

tube. Due to the unsteadiness of the flow, the average pressure in the plenum is lower than the stagnation pressure downstream of the inlet. The flow in the plenum oscillates due to the opening and closing of the valve during a cycle. An unsteady open-system control volume analysis was applied to the engine. Mass, momentum and energy equations were averaged over a cycle with no storage terms (steady flight conditions). The thrust of the engine is found to be the sum of three terms representing the detonation tube impulse, the ram momentum, and the ram pressure. Our single-cycle impulse model⁷ was modified to take into account the effect of detonation propagation into a moving flow generated by the filling process. The detonation tube impulse is found to decrease sharply with increasing filling velocity. Performance calculations were carried out for a PDE operating with hydrogen-air and JP10-air at 10,000 m altitude. The engine specific impulse is found to decrease quasi-linearly with increasing flight Mach number, and single-tube PDEs are found to generate thrust up to a flight Mach number of about 4. Comparison with conventional propulsion systems showed that the single-tube PDE in the configuration studied (straight detonation tube) operating with stoichiometric hydrogen- or JP10-air has a higher specific impulse than the ramjet below a flight Mach number of 1.35.

Acknowledgments

This work was supported by Stanford University Contract PY-1905 under Dept. of Navy Grant No. N00014-02-1-0589 *"Pulse Detonation Engines: Initiation, Propagation, and Performance"*.

References

- ¹Nicholls, J. A., Wilkinson, H. R., and Morrison, R. B., "Intermittent Detonation as a Thrust-Producing Mechanism," *Jet Propulsion*, Vol. 27, No. 5, 1957, pp. 534–541.
- ²Zhdan, S. A., Mitrofanov, V. V., and Sychev, A. I., "Reactive Impulse from the Explosion of a Gas Mixture in a Semi-infinite Space," *Combustion, Explosion and Shock Waves*, Vol. 30, No. 5, 1994, pp. 657–663.
- ³Zitoun, R. and Desbordes, D., "Propulsive Performances of Pulsed Detonations," *Combustion, Science and Technology*, Vol. 144, 1999, pp. 93–114.
- ⁴Harris, P. G., Farinaccio, R., Stowe, R. A., Higgins, A. J., Thibault, P. A., and Laviolette, J. P., "The Effect of DDT Distance on Impulse in a Detonation Tube," 37th AIAA/ASME/SAE/ASEE Joint Propulsion Conference and Exhibit, July 8–11, 2001, Salt Lake City, UT, AIAA 2001-3467.
- ⁵Cooper, M., Jackson, S., Austin, J., Wintenberger, E., and Shepherd, J. E., "Direct Experimental Impulse Measurements for Deflagrations and Detonations," *Journal of Propulsion and Power*, Vol. 18, No. 5, 2002, pp. 1033–1041.
- ⁶Endo, T. and Fujiwara, T., "A Simplified Analysis on a Pulse Detonation Engine," *Trans. Japan Soc. Aero. Space Sci.*, Vol. 44, No. 146, 2002, pp. 217–222.
- ⁷Wintenberger, E., Austin, J. M., Cooper, M., Jackson, S., and Shepherd, J. E., "An Analytical Model for the Impulse of a Single-Cycle Pulse Detonation Tube," *Journal of Propulsion and Power*, Vol. 19, No. 1, 2003.

- ⁸Kailasanath, K., Patnaik, G., and Li, C., "Computational Studies of Pulse Detonation Engine: A Status Report," 35th AIAA/ASME/SAE/ASEE Joint Propulsion Conference and Exhibit, June 20–24, 1999, Los Angeles, CA, AIAA 1999-2634.
- ⁹Brophy, C. M., Werner, L. S., and Sinibaldi, J. O., "Performance Characterization of a Valveless Pulse Detonation Engine," 41st AIAA Aerospace Sciences Meeting and Exhibit, January 6–9, 2003, Reno, NV, AIAA 2003-1344.
- ¹⁰Schauer, F., Stutrud, J., and Bradley, R., "Detonation Initiation Studies and Performance Results for Pulsed Detonation Engines," 39th AIAA Aerospace Sciences Meeting and Exhibit, January 8–11, 2001, Reno, NV, AIAA 2001-1129.
- ¹¹Kailasanath, K., "A Review of Research on Pulse Detonation Engine Nozzles," 37th AIAA/ASME/SAE/ASEE Joint Propulsion Conference and Exhibit, July 8–11, 2001, Salt Lake City, UT, AIAA 2001-3932.
- ¹²Wu, Y., Ma, F., and Yang, V., "System Performance and Thermodynamic Cycle Analysis of Air-Breathing Pulse Detonation Engines," *Journal of Propulsion and Power*, in print, 2003.
- ¹³Ma, F., Wu, Y., Choi, J. Y., and Yang, V., "Thrust Chamber Dynamics of Multi-Tube Pulse Detonation Engines," 41st AIAA Aerospace Sciences Meeting and Exhibit, January 6–9, 2003, Reno, NV, AIAA 2003-1168.
- ¹⁴Heiser, W. H. and Pratt, D. T., "Thermodynamic Cycle Analysis of Pulse Detonation Engines," *Journal of Propulsion and Power*, Vol. 18, 2002, pp. 68–76.
- ¹⁵Kentfield, J. A. C., "Fundamentals of Idealized Airbreathing Pulse-Detonation Engines," *Journal of Propulsion and Power*, Vol. 18, No. 1, 2002, pp. 77–83.
- ¹⁶Talley, D. and Coy, E., "Constant Volume Limit of Pulsed Propulsion for a Constant Gamma Ideal Gas," *Journal of Propulsion and Power*, Vol. 18, No. 2, 2002, pp. 400–406.
- ¹⁷Harris, P. G., Guzik, S., Farinaccio, R., Stowe, R. A., Whitehouse, D., Josey, T., Hawkin, D., Ripley, R., Link, R., Higgins, A. J., and Thibault, P. A., "Comparative Evaluation of Performance Models of Pulse Detonation Engines," 38th AIAA/ASME/SAE/ASEE Joint Propulsion Conference and Exhibit, July 7–10, 2002, Indianapolis, IN, AIAA 2002-3912.
- ¹⁸Quirk, J. J., "AMRITA - A Computational Facility (for CFD Modelling)," VKI 29th CFD Lecture Series, ISSN 0377-8312, 1998.
- ¹⁹Glass, I. I. and Sislian, J. P., *Nonstationary Flows and Shock Waves*, Clarendon Press, Oxford, 1994.
- ²⁰Culick, F. E. C. and Rogers, T., "The Response of Normal Shocks in Diffusers," *AIAA Journal*, Vol. 21, No. 10, 1983, pp. 1382–1390.
- ²¹Yang, V. and Culick, F. E. C., "Analysis of Unsteady Inviscid Diffuser Flow with a Shock Wave," *Journal of Propulsion and Power*, Vol. 1, No. 3, 1985, pp. 222–228.
- ²²Mullagiri, S., Segal, C., and Hubner, P. J., "Oscillating Flows in a Model Pulse Detonation Engine," *AIAA Journal*, Vol. 41, No. 2, 2003, pp. 324–326.
- ²³Hill, P. G. and Peterson, C. R., *Mechanics and Thermodynamics of Propulsion*, Addison-Wesley, Second Edition, 1992.
- ²⁴Thompson, P. A., *Compressible Fluid Dynamics*, Advanced Engineering Series, Rensselaer Polytechnic Institute, pp. 347–359, 1988.
- ²⁵Mattingly, J. D., Heiser, W. H., and Daley, D. H., *Aircraft Engine Design*, AIAA Education Series, 1987.
- ²⁶Reynolds, W., "The Element Potential Method for Chemical Equilibrium Analysis: Implementation in the Interactive Program STANJAN," Tech. rep., Mechanical Engineering Department, Stanford University, 1986.
- ²⁷Wintenberger, E., Austin, J. M., Cooper, M., Jackson, S., and Shepherd, J. E., "Impulse of a Single-Pulse Detonation Tube," Tech. rep., Graduate Aeronautical Laboratories, California Institute of Technology, 2002, Report FM00-8.
- ²⁸*Aviation Fuel Properties*, Coordinating Research Council, 1983, CRC Report No. 530.